O. Hahtela, N. Chekurov and I. Tittonen, Non-tilting out-of-plane mode high-*Q* mechanical silicon oscillator, Journal of Micromechanics and Microengineering 15, 1848-1853 (2005).

© 2005 Institute of Physics Publishing

Reprinted with permission.

http://www.iop.org/journals/jmm

INSTITUTE OF PHYSICS PUBLISHING JOURNAL OF MICROMECHANICS AND MICROENGINEERING

J. Micromech. Microeng. **15** (2005) 1848–1853 doi:10.1088/0960-1317/15/10/009

Non-tilting out-of-plane mode high-Q mechanical silicon oscillator

O Hahtela[1,2], **N Chekurov**[1,2] **and I Tittonen**[1,2]

[1] Optics and Molecular Materials, Micronova, Helsinki University of Technology, PO Box 3500, FIN-02015 TKK, Finland
[2] Center for New Materials, Helsinki University of Technology, Espoo, Finland

E-mail: ossi.hahtela@tkk.fi

Received 25 April 2005, in final form 23 June 2005
Published 9 August 2005
Online at stacks.iop.org/JMM/15/1848

Abstract

A single-crystal silicon oscillator with a non-tilting out-of-plane vibrational mode and high-quality factor for the mechanical resonance was designed, fabricated and characterized. The finite-element method (FEM) was utilized before the fabrication process to simulate the oscillator behavior and give guidance in optimizing the design. At low pressure $p = 10^{-3}$ mbar and at room temperature, the resonance frequency and Q value were measured to be $f_0 = 26\,526$ Hz and $Q = 100\,000$, respectively. The measured resonance frequency was in a good agreement with the simulated one, $f_{0,\mathrm{FEM}} = 26\,787$ Hz. The actual mode pattern was verified by measurements and compared with the simulation result. An interferometric laser beam was scanned over the oscillator surface and position-dependent oscillation amplitudes were stored with the phase-sensitive detection. The oscillation was proved to occur effectively in a pure non-tilting out-of-plane mode. We propose to use this kind of micromechanical probe in various measurement schemes, where one needs to approach the surface with a single non-torsional plane. In addition, such an oscillator can be utilized as an optical mirror so that the optical mode can be kept the same when moving the mirror.

1. Introduction

Mechanical oscillators contain elements that typically vibrate in flexural (deflection), torsional or longitudinal (extensional, bulk) modes [1–3]. High mechanical quality (Q value) of the resonance is desired in many high precision sensing applications. Torsionally vibrating structures have proved to be successful solutions for designing high-Q oscillators [2, 4, 5]. In these structures, one idea has been to use balanced designs so that the center of mass of the oscillator is stationary in a torsional mode, which leads to very small intrinsic energy losses [6].

Torsional motion, however, is not always optional because of the inherent tilting of oscillation. In some physical experiments it is desirable that the motion of a mechanical oscillator takes place precisely in a direction that is normal to the oscillator surface. For example, if a torsional mechanical oscillator is employed as a mirror in an interferometric system [7–9], torsional motion inevitably introduces deflection of the reflected light and makes an optical mode stabilization impossible. In principle, the excitation of a torsional oscillation requires a torsional force, i.e. torque, on the oscillator. This may set limitations to the type of force that can be detected with a torsional oscillator. For example, if the studied force can be considered as a plane wave with a large cross-section compared to the oscillator surface area, the torsional oscillation mode may not become excited. When studying the short-range interaction of surfaces, such as Casimir force of two conducting plates [10] with a micromechanical oscillator, the oscillating element should be kept parallel to the other surface. In addition, such experiments typically require very small separation between the surfaces which limits the use of torsional motion to a certain extent.

In this work, we demonstrate a mechanical silicon oscillator structure vibrating effectively in a non-tilting out-of-plane mode and having a resonance frequency of $f_0 = 26.5$ kHz. The oscillator exploits a supporting structure which still allows a balanced oscillation mode, very low clamping losses and thus very high mechanical Q value ($Q = 100\,000$) in vacuum at room temperature.

 © 2005 IOP Publishing Ltd Printed in the UK

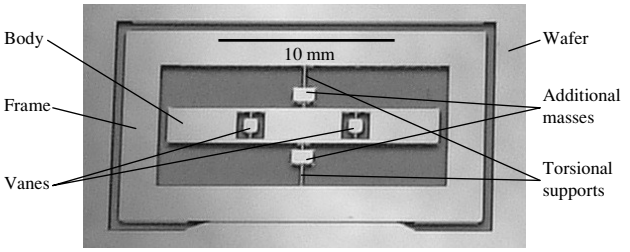

Figure 1. A photograph of the microfabricated non-tilting out-of-plane mode oscillator. Here the oscillator is still attached to the silicon wafer.

2. Non-tilting out-of-plane mode high-Q oscillator

2.1. Oscillator design

The microfabricated out-of-plane mode high-Q mechanical silicon oscillator used in this work is illustrated in figure 1. The elements of the oscillator structure vibrating in a non-tilting mode are the two rectangular silicon vanes with the size of $0.8 \times 0.8 \times 0.38$ mm^3. These vanes are mounted with narrow bridges to the oscillator body ($1.5 \times 14 \times 0.38$ mm^3) which is basically a free–free beam vibrating in a second flexural mode. The mounting of the vanes is accurately positioned to the antinodes of the oscillator body. This arrangement guarantees that the two vibrating vanes are in anti-phase relative to each other and precisely parallel to their equilibrium position (i.e. yz plane) during the whole vibration cycle.

The oscillator support always causes some leakage of mechanical energy. In order to minimize these energy losses, the support arrangement must be carefully designed. We use two torsional suspension bars to mount the oscillator body to the frame. Torsional bars are located on the oscillator body symmetry axis, i.e. at the oscillation node, which allows good isolation of vibrational energy [11]. Ideally the suspension bars experience only torsional motion in the high-Q mode oscillation. The lengths of these bars are chosen to correspond to the effective quarter wavelength of the resonance frequency of the oscillator body. Thus, the suspension bars act as impedance matched acoustic transmission lines and the oscillator body experiences minimum energy dissipation through the support [1]. The advantage of inserting additional masses on the thin torsional suspension bars is that one can use shorter suspension bars and gain a mechanically robust structure.

2.2. Fabrication of the oscillators

Oscillators were fabricated from a double-sided polished, 380 μm thick (1 0 0) oriented single-crystal silicon wafer (p type, 5–10 Ω cm). Single-crystal silicon has excellent elastic properties and very low intrinsic losses which make it an appropriate material for high-Q oscillators [12]. A thermal silicon oxide layer was grown on the wafer to be used as an etch mask. Structures were released by double-sided anisotropic wet etching in a 25% TMAH solution at 85 °C. This fabrication process has the benefit of allowing well-defined symmetric features and high surface quality which are needed for reaching balanced oscillation mode and low damping. The polished silicon surface provides a power reflection constant of $R = 0.34$ for the HeNe-laser wavelength, allowing silicon components to be used as low-reflectivity mirrors in optical measurements.

2.3. Oscillator mechanical model

If the surrounding openings of the vanes are excluded, the oscillator body can be considered as a uniform free–free beam which vibrates in the second flexural mode. The characteristic function $x_n(y)$ gives the mode pattern (i.e. the oscillation amplitudes along the y-axis) of the nth oscillation mode [13]:

$$x_n(y) = A_n[(\cos\beta_n L - \cosh\beta_n L)(\sin\beta_n y + \sinh\beta_n y) - (\sin\beta_n L - \sinh\beta_n L)(\cos\beta_n y + \cosh\beta_n y)], \quad (1)$$

where A_n is a constant, L is the length of the free–free beam and $\beta_n L$ is a parameter related to the nth flexural mode of the free–free beam. For the second flexural mode $\beta_2 L = 7.8532$.

The mechanical oscillator discussed in this paper can be modeled as a one-dimensional harmonic oscillator characterized by an effective mass m_{eff}, angular resonance frequency ω_0 and mechanical quality Q. Angular resonance frequency for a high-Q oscillation mode is determined by its spring constant k and effective mass, $\omega_0 = 2\pi f_0 = (k/m_{\mathrm{eff}})^{1/2}$. The equation of motion of a damped harmonic mechanical oscillation under the external monochromatic driving force $F(t)$ with angular frequency ω can be written as

$$m_{\mathrm{eff}}\frac{\mathrm{d}^2x}{\mathrm{d}t^2} + \frac{m_{\mathrm{eff}}\omega_0}{Q}\frac{\mathrm{d}x}{\mathrm{d}t} + m_{\mathrm{eff}}\omega_0^2 x = F_0\cos(\omega t), \quad (2)$$

where $x(t)$ is the oscillator displacement as a function of time. The solution of $x(t)$ is given by [14]

$$x(t) = x_0\,\mathrm{e}^{-\frac{\omega_0 t}{2Q}}\cos(\omega t + \alpha) + |\chi(\omega)|F_0\cos[\omega t + \delta(\omega)], \quad (3)$$

where the first term on the right-hand side is the transient part of the oscillator response (exponentially damped harmonic oscillation), x_0 is the oscillation amplitude and α is the phase shift. The second term is the steady-state part of the solution (frequency response of the oscillation) and $\chi(\omega)$ is the mechanical susceptibility with Lorentzian behavior,

$$\chi(\omega) = \frac{1}{m_{\mathrm{eff}}\left(\omega_0^2 - \omega^2 - \mathrm{i}\omega\omega_0/Q\right)}. \quad (4)$$

The frequency response of phase $\delta(\omega)$ can be written as [14]

$$\tan[\delta(\omega)] = \frac{\omega\omega_0}{Q\left(\omega^2 - \omega_0^2\right)}. \quad (5)$$

3. Finite-element model simulation

Before the component fabrication, a three-dimensional finite-element model of the oscillator was utilized to inspect the out-of-plane vibrational high-Q mode. Although the exact numerical Q value cannot be predicted by finite-element simulation, it is a convenient method to estimate the damping of mechanical energy in different vibrational modes because it reveals the strain concentration and stress maxima points generated in the oscillator structure. Therefore, finite-element modeling can be used to give guidance in optimizing oscillator design for obtaining low damping [15].

The finite-element modeling used here contains some simplifications and inaccuracies. The cross-section of the

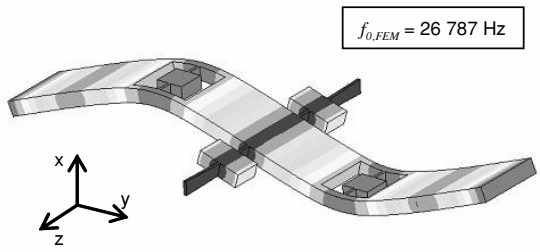

Figure 2. The non-tilting out-of-plane high-Q oscillation mode given by the FEM simulation. Position-dependent displacements in the x-direction are largely exaggerated. The surrounding frame of the oscillator is not shown here.

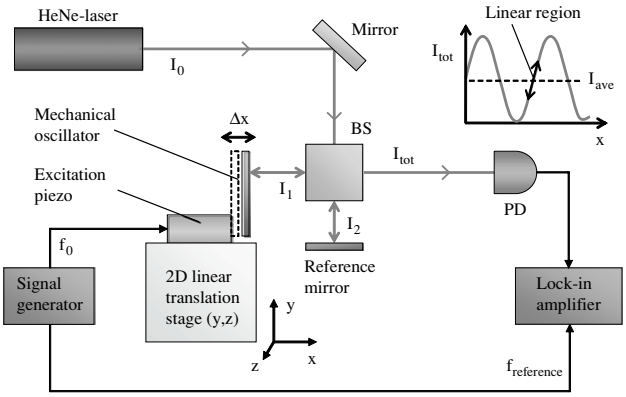

Figure 3. A Michelson interferometer configuration was used to measure the position-dependent oscillation amplitudes and to verify the actual mode pattern of the non-tilting high-Q oscillation mode.

oscillator was modeled as rectangular and the influence of the oblique side walls due to the double-sided anisotropic wet etching was neglected. Moreover, small variations in etching the corner compensation structures may result in slightly inaccurate shapes of the outer corners. The result of the simulation of the non-tilting high-Q oscillation mode pattern is illustrated in figure 2. The frame of the oscillator is not shown in the figure. The position-dependent displacements in the x-direction are largely exaggerated. The simulated resonance frequency of the high-Q mode was $f_{0,\mathrm{FEM}} = 26\,787$ Hz.

4. Measurement setup

The measurement setup is shown in figure 3. The oscillator was clamped by pressing the short edge of the frame between two aluminum parts. Energy losses at the clamping were estimated to be negligible since, according to the FEM simulations and measurements, the clamping area is well decoupled from the high-Q oscillation. The oscillator mount was attached to a two-dimensional translation stage which allows an accurate control of the oscillator position in the y- and z-directions.

The actuation of the oscillator was mechanically realized by using a signal generator driven piezo transducer which was attached to the oscillator mount. The signal generator also provides a reference signal for the phase-sensitive detection of a lock-in amplifier. The signal generator and the lock-in amplifier are connected to a computer for storing the measurement data and controlling the oscillator actuation through a feedback loop. The computer control that was used in this work allowed either an automated excitation frequency sweep over desired bandwidth or locking the exciting signal to the oscillator resonance frequency.

Gas damping of the surrounding medium is the main source of energy losses of high-Q mechanical oscillation. Thus, the oscillator was placed in a vacuum chamber for detecting the maximum reachable Q value. The turbo-molecular pump created low pressures down to $p = 10^{-5}$ mbar. This pressure is low enough since gas damping is negligible under $p = 10^{-3}$ mbar [11].

In this work, a HeNe-laser beam was utilized as an interferometric probe to detect the displacements in the oscillator position in the x-direction (figure 3). We used a Michelson interferometer configuration in which the mechanical silicon oscillator was acting as a moving mirror in one of the interferometer arms. The stationary reference mirror utilized in the other interferometer arm is also a piece of polished silicon so that the two reflected interfering light fields have similar intensities, $I_1 = I_2$, giving the maximum modulation depth at the output.

The output intensity of the Michelson interferometer I_{out} depends on the position of the movable mirror relative to the stationary reference mirror as the phase difference between the two reflected light fields is changed. The output intensity is

$$I_{\mathrm{out}}(\Delta x) = \frac{R}{2}\left[I_0 + I_0 \cos\left(\frac{4\pi\,\Delta x}{\lambda}\right)\right], \qquad (6)$$

where R is the power reflection constant of the polished silicon surface, I_0 is the intensity of the incident light and the beamsplitter is considered lossless. In order to guarantee that the interferometer response occurs in the linear region (figure 3), the equilibrium position of the oscillator must correspond to the average output intensity I_{ave}, and the oscillation amplitude Δx must be small compared to the wavelength of the used light ($\Delta x \ll \lambda$). Therefore, an additional piezo-driven translation stage is utilized to control the oscillator equilibrium position in the x-direction and the strength of the oscillator excitation is kept at a moderate level. Interferometer output is detected with a silicon photodiode and monitored by a dual-phase lock-in amplifier.

The oscillator displacements were measured with high resolution comparable to a small fraction of the wavelength of light. The measurement sensitivity was determined to be $S_x^{\frac{1}{2}} = 5.6 \times 10^{-13}$ m Hz$^{-\frac{1}{2}}$. The optical interferometric measurement method used in this work was proved to be an accurate and flexible tool to perform vibrational analysis of a microfabricated silicon component. Surface scanning by altering the position of the laser probe beam in the yz plane with the two-dimensional translation stage gives possibilities of measuring the position-dependent oscillator displacements and thus generating the vibrational mode pattern of the oscillation.

5. Measurements

5.1. Verification of the mode pattern

The actual non-tilting out-of-plane oscillation mode pattern was verified by measurements because additional spurious

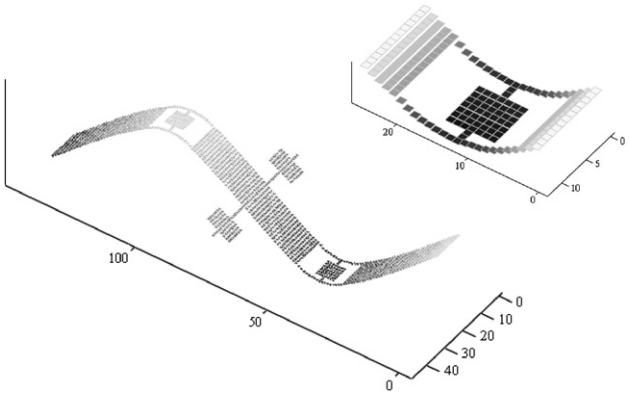

Figure 4. The actual mode pattern was verified by measurements. The inset shows an enlarged picture of one of the oscillator vanes.

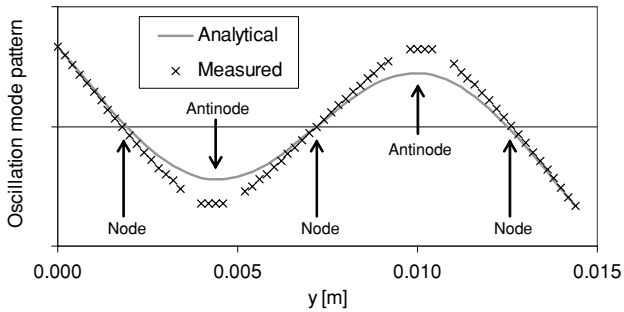

Figure 5. The normalized analytical solution of the second flexural mode of the uniform free–free beam and measured mode pattern along the y-axis. The openings around the vanes reduce the oscillator stiffness in the neighborhood of the antinodes.

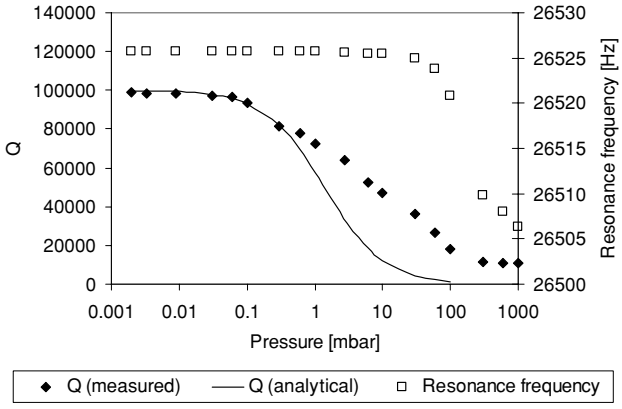

Figure 6. The measured Q value and resonance frequency as functions of pressure at room temperature. In comparison, the solid line shows the pressure dependence of the Q value of a uniform resonant beam at low pressures according to a theoretical model given in [17].

vibrational modes could degenerate the oscillator performance if coupled to the desired high-Q mode. The shape of the vanes implies that they possess a torsional oscillation mode as well. However, the resonance frequency of the non-tilting out-of-plane oscillation is determined by the resonance frequency of the second flexural mode of the oscillator body ($f_0 = 26.5$ kHz) and is thus significantly far from that of the torsional mode of the vanes. Torsional mode of the vanes occurs at a frequency of $f_{0,\mathrm{to}} \approx 1$ MHz and is well decoupled from the non-tilting out-of-plane oscillation mode. Longitudinal and torsional vibration modes of the body were concluded not to affect the desired high-Q resonance mode because the first-order longitudinal and torsional modes occur at approximately one order of magnitude higher frequencies than the second flexural mode of the body. Another possible spurious oscillation mode is, e.g., the one in which the torsional suspension bars have an additional flexural motion causing the oscillator support area to vibrate like a trampoline in a direction perpendicular to the initial component surface, i.e. the yz plane [1]. Also this mode was noted to be satisfactorily separated from the desired out-of-plane mode.

The measured oscillation mode pattern was composed by scanning the interferometer probe beam over the oscillator area in the y- and z-directions and reading the position-dependent interferometer response which is proportional to the magnitude of the oscillation amplitude (figure 4). The scanning was realized by using two orthogonally situated micrometer translation stages, and 100 μm steps in the y- and z-directions were used. Each small square in figure 4 corresponds to one measurement point and an area of $100 \times 100\ \mu\mathrm{m}^2$. The grayscale of the square is directly proportional to the oscillation amplitude of the oscillator at the corresponding coordinate. The simulated and measured results of the high-Q mode pattern are in a very good agreement with each other (figures 2 and 4).

Each rectangular vane was measured in total at 49 locations (inset of figure 4). The oscillation amplitude at each measured location across the vane was 10 nm $\pm$ 50 pm. This small uncertainty in the measured oscillation amplitudes indicates that the vanes oscillate in a pure non-tilting out-of-plane mode and that the torsional motion, flexural deformation of the vanes and other higher order modes are sufficiently suppressed. It should be noted that the roughness of a highly polished silicon wafer is at best of the order of a few angstroms and much larger than the uncertainty in the measured parallelism of the vibrating vanes. Therefore, it can be concluded that the mode purity of our non-tilting out-of-plane mode high-Q oscillator is excellent for applications that require parallel approaching of the surfaces to very small distances.

In addition, the measured mode pattern was compared to the analytical solution of the uniform free–free beam given in equation (1). The normalized mode patterns along the y-axis are illustrated in figure 5. The surrounding openings of the vanes introduce a local decrease in the stiffness of the oscillator body in the neighborhood of the antinodes. This can be seen as a sharper bending of the oscillator body.

5.2. Oscillator characterization at low pressure

The resonance frequency and the Q value were determined as functions of pressure at room temperature. The interferometric probe beam was pointed to the center of the rectangular vane and the interferometer response was monitored with a lock-in amplifier. Measurement results are shown in figure 6.

The damping at very low pressures is determined e.g. by internal energy dissipation mechanisms and clamping losses [2]. In the intrinsic damping region ($p < 0.01$ mbar) the

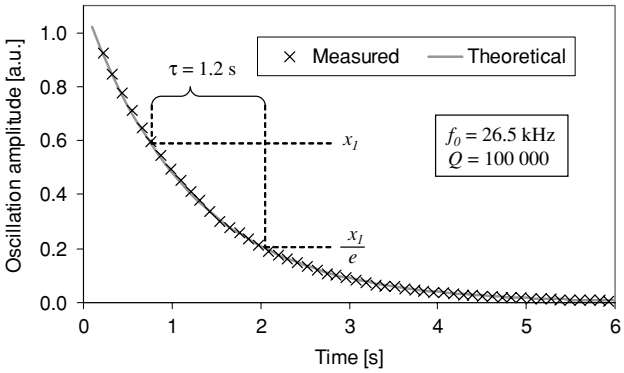

Figure 7. The measured and theoretically calculated decay curves of the high-Q oscillation mode at $p = 10^{-3}$ mbar and room temperature.

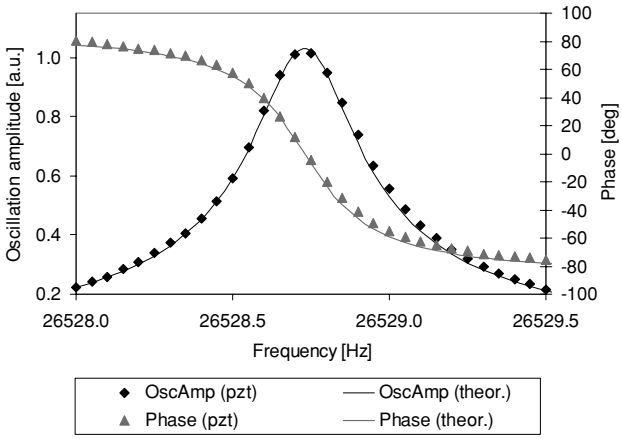

Figure 8. Frequency responses of the oscillation amplitude and phase at $p = 0.1$ mbar and room temperature. The high-Q mode was excited mechanically by a piezo actuator (pzt). The solid lines refer to the frequency responses according to equations (3) and (5).

mechanical quality of the non-tilting out-of-plane mode was measured to be $Q_0 = 100\,000$. As the pressure is increased the increasing number of individual gas molecules hitting the oscillator surface introduces additional molecular damping. In the molecular damping region the Q value of resonant beam structures is typically inversely proportional to the pressure, $Q(p) \propto p^{-1}$ [2, 16, 17]. In comparison, the solid line in figure 6 illustrates the pressure dependence of the Q value which is calculated by using a theoretical model for damping of a uniform resonant microbeam given in [17]. Above 1 mbar the measured Q values are clearly higher than the calculated Q values. One explanation for the reduced molecular damping is the fact that a fraction of the gas molecules drifts through the openings of the vanes instead of hitting the surface as in the case of a uniform beam. In the viscous damping region ($p > 100$ mbar) the surrounding gas acts as a viscous fluid and the Q value was measured to be $Q_{\mathrm{vis}} = 10\,600$.

The resonance frequency was measured to be $f_0 = 26\,526$ Hz in vacuum being in a rather good agreement with the simulated one, $f_{0,\mathrm{FEM}} = 26\,787$ Hz. It was demonstrated that the resonance frequency shows pressure dependence at pressures exceeding 10 mbar. The pressure dependence of the resonance frequency due to gas damping, $f_m(p) = f_0[1–1/4Q(p)^2]^{\frac{1}{2}}$, at even higher pressures is negligible for high-Q oscillators.

5.3. Decay time measurement

Oscillator was mechanically excited to vibrate at its resonance frequency by using a piezo actuator attached to the oscillator mount. The resulting oscillation amplitude saturates to the equilibrium level. At this oscillation level the external excitation energy and energy losses of the oscillator are in balance. The oscillation amplitude was measured from the center of the vane. When the excitation was switched off, the oscillation started decaying (ringing down) and the envelope curve of the exponentially damped oscillation was stored with a lock-in amplifier (figure 7). The Q value can be determined from the resonance frequency f_0 and decay time τ corresponding to the oscillation amplitude being decreased to (1/e)th part of its initial value, $Q = \pi \tau f_0$. The solid line in figure 7 illustrates the exponential decay curve which was calculated by using the transient part of equation (3) and experimentally determined numerical values of $f_0 = 26\,526$ Hz, $x_0 = 1.1$ nm and $Q = 100\,000$.

5.4. Frequency response measurement

Frequency response of the oscillation amplitude of a mechanical resonance has a clear Lorentzian behavior as described by the steady-state part of equation (3). The frequency response was measured by sweeping the excitation frequency over the resonance and storing the resulting oscillation amplitude and phase with the lock-in amplifier (figure 8). The probe beam was pointed to the center of the vane. Excitation was kept at a moderate level in order to guarantee that the resonance peak is symmetric and to avoid hysteresis behavior. It can be seen that the measured frequency response of the oscillation amplitude is close to a single Lorentzian curve and therefore similar to the one calculated by using the steady-state part of equation (3). Here the measured numerical values of f_0 and Q were used and the parameter F_0/m_{eff} was normalized so that the calculated oscillation amplitude corresponds to the measured one at resonance. Also the phase response in figure 8 behaves as predicted in equation (5).

6. Conclusions

A carefully designed high-Q mechanical silicon oscillator vibrating in a non-tilting out-of-plane mode was presented in this work. The oscillator was measured to have a resonance frequency of $f_0 = 26.5$ kHz and a Q value of 100 000 at low pressure $p < 10^{-2}$ mbar and at room temperature. Three-dimensional finite-element method simulation was demonstrated to give accurate predictions of the resonance frequency and vibrational mode pattern. It was shown that the non-tilting high-Q oscillators can be produced by combining appropriate oscillator material, balanced oscillation mode and low loss support. In order to minimize energy losses at the support, quarter wavelength torsional suspension bars were used to mount the oscillator structure at the nodal points.

Oscillators with a non-tilting out-of-plane vibrational mode can offer very low damping of mechanical energy

and thus show strong potential for high precision sensing applications. It was shown that the oscillation occurs in a pure non-tilting out-of-plane mode and, therefore, our oscillator designs are suitable to be used e.g. as moving mirrors in interferometric systems. Further applications can be found in those experiments that require parallel approaching of the surface to very short distances as in AFM, micro bridges, Kelvin probe, gas detection and in short range detection of weak forces.

Many high precision sensing applications may benefit from the utilization of oscillators with higher resonance frequency and smaller mass. The resonance frequency of our out-of-plane mode high-Q oscillator is inversely proportional to the body length if the aspect ratio is kept constant. In miniaturization of our design, a scaling factor of 1:50 seems very realistic if the components were fabricated e.g. by using silicon-on-insulator (SOI) technology. Unfortunately, intrinsic damping increases when the size of the oscillator is reduced [6, 18]. The surface contribution to total losses is significant and, therefore, the increased surface-to-volume ratio may lead to a reduced Q value. In any case, much higher resonance frequencies of the order of MHz can be achieved.

References

[1] Wang K, Wong A-C and Nguyen C T-C 2000 VHF free–free beam high-Q micromechanical resonators *J. Microelectromech. Syst.* **9** 347–60

[2] Buser R A and de Rooij N F 1990 Very high Q-factor resonators in monocrystalline silicon *Sensors Actuators* A **21–23** 323–7

[3] Mattila T, Kiihamäki J, Lamminmäki T, Jaakkola O, Rantakari P, Oja A, Seppä H, Kattelus H and Tittonen I 2002 A 12 MHz micromechanical bulk acoustic mode oscillator *Sensors Actuators* A **101** 1–9

[4] Kleiman R N, Kaminsky G K, Reppy J D, Pindak R and Bishop D J 1985 Single-crystal silicon high-Q torsional oscillators *Rev. Sci. Instrum.* **56** 2088–91

[5] Liu X, Morse S F, Vignola J F, Photiadis D M, Sarkissian A, Marcus M H and Houston B H 2001 On the modes and loss mechanisms of a high-Q mechanical oscillator *Appl. Phys. Lett.* **78** 1346–8

[6] Lifshitz R and Roukes M L 2000 Thermoelastic damping in micro- and nanomechanical systems *Phys. Rev.* B **61** 5600–9

[7] Caves C M 1980 Quantum-mechanical radiation-pressure fluctuations in an interferometer *Phys. Rev. Lett.* **45** 75–9

[8] Tittonen I, Breitenbach G, Kalkbrenner T, Müller T, Conradt R, Schiller S, Steinsland E, Blanc N and de Rooij N F 1999 Interferometric measurements of the position of a macroscopic body: towards observation of quantum limits *Phys. Rev.* A **59** 1038–44

[9] Hahtela O, Nera K and Tittonen I 2004 Position measurement of a cavity mirror using polarization spectroscopy *J. Opt. A: Pure Appl. Opt.* **6** S115–20

[10] Chan H B, Aksyuk V A, Kleiman R N, Bishop D J and Capasso F 2001 Nonlinear micromechanical Casimir oscillator *Phys. Rev. Lett.* **87** 211801

[11] Mihailovich R E and MacDonald N C 1995 Dissipation measurements of vacuum-operated single-crystal silicon microresonators *Sensors Actuators* A **50** 199–207

[12] Petersen K E 1982 Silicon as a mechanical material *Proc. IEEE* **70** 420–57

[13] Meirovitch L 1967 *Analytical Methods in Vibrations* (New York: Macmillan)

[14] Spiel C L, Pohl R O and Zehnder A T 2001 Normal modes of a Si(100) double-paddle oscillator *Rev. Sci. Instrum.* **72** 1482–91

[15] Beeby S P and Tudor M J 1995 Modelling and optimization of micromachined silicon resonators *J. Micromech. Microeng.* **5** 103–5

[16] Newell W E 1968 Miniaturization of tuning forks *Science* **161** 1320–6

[17] Li B, Wu H, Zhu C and Liu J 1999 The theoretical analysis on damping characteristics of resonant microbeam in vacuum *Sensors Actuators* A **77** 191–4

[18] Yasumura K Y, Stowe T D, Chow E M, Pfafman T, Kenny T W, Stipe B C and Rugar D 2000 Quality factors in micron- and submicron-thick cantilevers *J. Microelectromech. Syst.* **9** 117–25